Application of FMS images in poorly recovered coring intervals: examples from ODP Leg 129

A. R. M. SALIMULLAH & D. A. V. STOW

Geology Department, The University, Southampton SO9 5NH, UK

Abstract. A thick sedimentary section was penetrated at three sites in the West Central Pacific during the Ocean Driling Program (ODP) Leg 129. Although average core recovery ranged from 17.3 to 29.5%, recovery in some intervals falls as low as 0–5%. Furthermore, the recovered portion of the core is conventionally assigned to the topmost part of the cored interval, although this is now known to be incorrect in most instances in consolidated parts of the section. These drawbacks have led to incomplete and even erroneous sedimentological interpretations. High-resolution electrical (Formation MicroScanner) images of the borehole obtained by scanning the borehole wall with arrays of small electrodes pressed against the borehole surface can provide:

(1) detailed sedimentary structure and texture of missing sections of each core, through calibration with visual data obtained from recovered cores;
(2) the original sedimentary features, where these have been disturbed or brecciated during drilling, as well as drilling artifacts on the borehole wall;
(3) recognition of sedimentary facies (e.g. slump units in hole 801B) in non-recovered intervals;
(4) correct location of recovered portions within the cored interval, through matching of specific sedimentary features.

Examples of these applications of the FMS images to the poorly recovered ODP Leg 129 cores are presented. The use of FMS logging has widespread application in any borehole where conventional cores have not been taken or where core recovery is limited. However, log calibration with core samples is essential.

Three sites were drilled during the Ocean Drilling Program (ODP) Leg 129; Sites 800 and 801 in Pigafetta Basin and Site 802 in East Mariana Basin (Fig. 1). A thick sedimentary section was penetrated at each of the sites and the summary lithostratigraphy (Shipboard Scientific Party 1990) is shown in Fig. 2. For this study, the Cretaceous and Mio-Pliocene volcaniclastic Units of sites 801 and 802 are considered. These were deposited in a typical mid-ocean plate setting in an area surrounded by volcanic seamounts that showed intense activity at different periods of ocean development. The full range of resedimentation processes, including slumps,

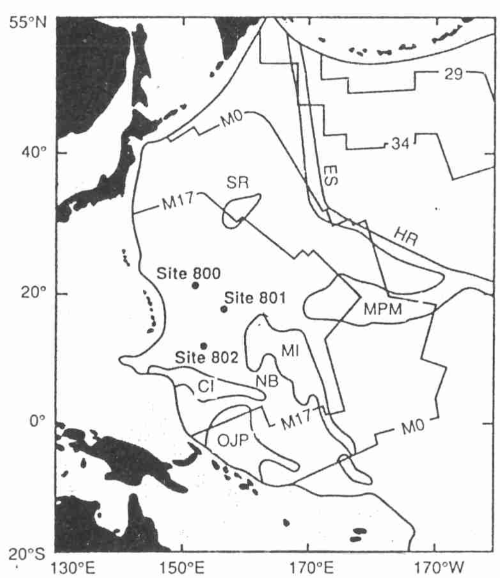

Fig. 1. Location of Leg 129 sites 800, 801 and 802. Bedrock isochromes are determined from magnetic anomaly lineation mapping on the Pacific plate (after Larson *et al.* 1985) and superimposed on groups of islands, atolls, and guyots in the western Pacific Ocean. (Feature abbreviations are as follows: Caroline Islands (CI), Ontong Java Plateau (OJP), Marshall Islands (MI), Nauru Basin (NB), Mid-Pacific Mountains (MPM), Shatsky Rise (SR), Hawaiian Ridge (HR), and Emperor Seamounts (EM). Jagged contours represent magnetic lineations and unshaded areas represent normal Pacific oceanic crust. Shaded areas represent volcanic edifices with thickened crustal sections, as well as the younger areas beyond the Pacific subduction zones).

From HURST, A., GRIFFITHS, C. M. & WORTHINGTON, P. F. (eds), 1992, *Geological Applications of Wireline Logs II*. Geological Society Special Publication No. 65, pp. 71–86.

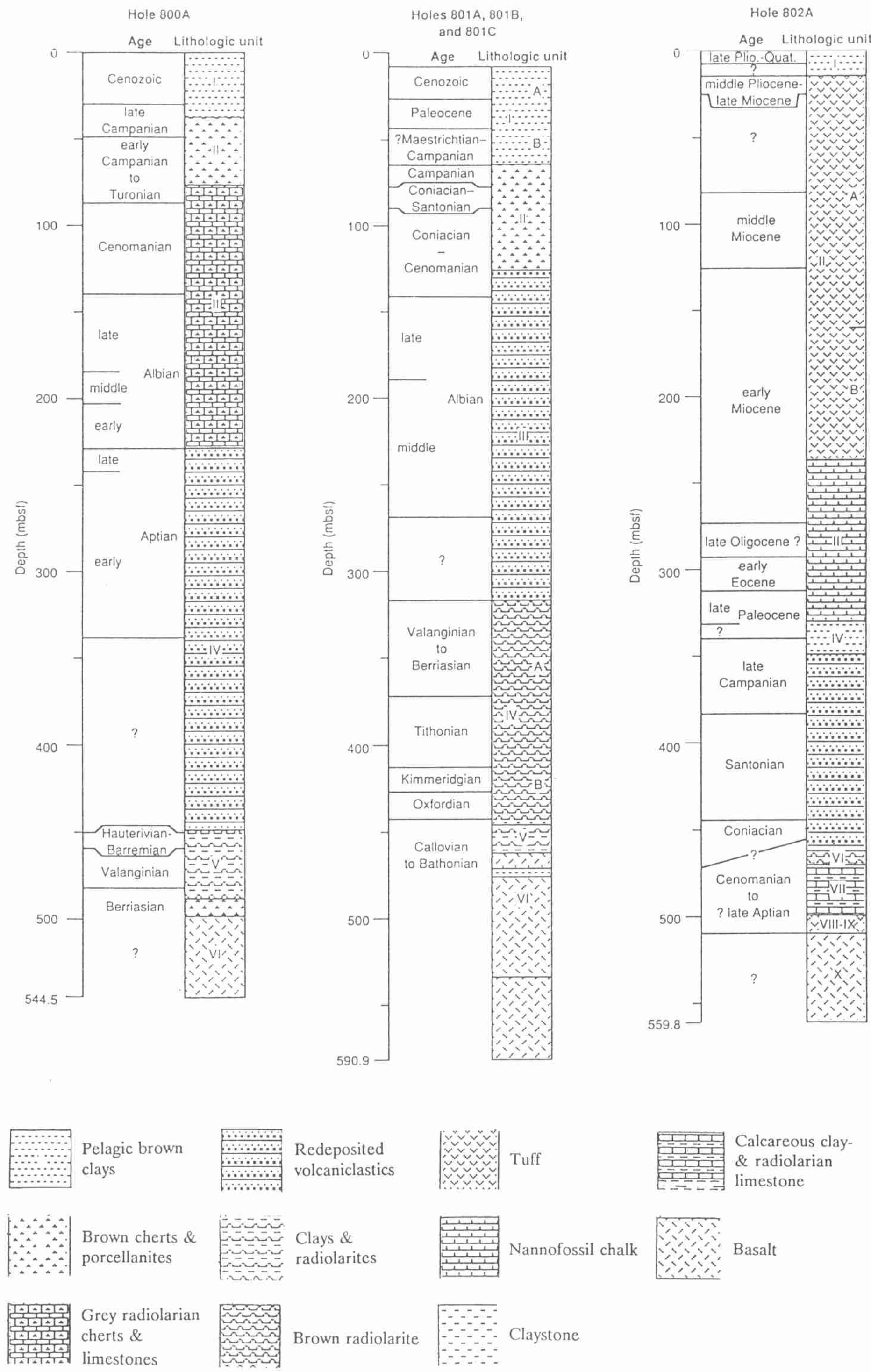

Fig. 2. Summary lithostratigraphic columns for ODP Leg 129 (from Shipboard Scientific Party 1990).

debris flows and turbidity currents (Salimullah & Stow, this volume) were responsible for the reworking of material from the flanks of seamounts and their input into the adjacent basins. Background pelagic sedimentation was mainly radiolarian-rich in the Pigafetta Basin and nannofossil or clay-rich in the East Mariana Basin.

As is commonly the case with unconsolidated cohesionless sediments, core recovery was very poor, as little as 0–5% in some intervals. The borehole walls have most probably suffered disruption as a result of caving and washout, and portions of cores that were recovered are typically abraded, fragmented and brecciated due to drilling disturbance. However, a good suite of logs was taken at two of the sites, and the specific objective of this study is to demonstrate how the FMS images can be used to:

(a) delineate detailed sedimentary features in intervals with poor core recovery;

(b) delineate the original sedimentary features where these have been abraded or brecciated during drilling;

(c) recognize sedimentary facies in non-recovered coring intervals;

(d) assign the correct location of short-length recovered portions within the known cored interval.

FMS tool and image processing

The FMS tool (Fig. 3) is capable of producing high-resolution borehole images from electrical conductivity measurements. Although it has been used in the petroleum industry since 1986, its use in the ODP has been constrained by the narrow internal diameter (10.48 cm) of the drill pipe used on the *Joides Resolution* drillship (Shipboard Scientific Party 1990). Consequently, a modified sensor was developed by Schlumberger for ODP use. This sensor was designed in such a way that four images (of 16 traces each), instead of two images obtained in the original version of Schlumberger (Ekstrom *et al.* 1986) are recorded simultaneously (Shipboard Scientific Party 1989).

The button current intensity (raw data points) is sampled every 2.5 mm (Serra 1989) by the FMS. This contrasts markedly with most conventional downhole measurements that are usually sampled at 150 mm; hence the sampling rate of the FMS is 60 times larger than that of most other logging devices.

Once the data have been acquired in the borehole, the images are processed and enhanced (for details see Serra 1989). Various image enhancement methods can be applied. Different sizes of sliding window are used to improve the local contrast of an image in order to delineate finer details of an event (Serra 1989) such as distribution of clasts (larger than 1 cm) in beds of debrites. For this study, dynamic and 'hilite' normalization images are used. All the 'hilite' images were processed with a 20 cm sliding window and the dynamic images with 10 and 30 cm windows (sliding window size is mentioned for each image in the respective figure caption).

The FMS has an imaging resolution of the order of a few millimetres in both vertical and azimuthal directions (Ekstrom *et al.* 1986). Sedimentary features as small as 1.2 cm can therefore be resolved on the FMS images (Harker *et al.* 1990).

Image interpretation approach and grading

The poor/non-recovery of cores as well as degree of disturbance of recovered-cores and of the borehole wall due to drilling, makes the direct calibration of FMS images difficult. Nevertheless, the recovered material does provide some information on sediment texture, structure, composition, grain density, porosity and water content with which to interpret the images as well as to interpolate and/or extrapolate that interpretation to poorly recovered intervals. In these cases, it is not possible to ascertain the primary control(s) on the scale of grey levels of the images. However, the situation is far better in well-recovered coring intervals where direct calibration of images reveals that the grey scale of the images is largely controlled by grain size. In other words, the image becomes increasingly darker grey with an increase in the amount of clay-size material, as is also observed in siliciclastic rocks (Serra 1989). The change in grain size through a graded bed, for example, is typically accompanied by a slight change in composition (mineralogy), water content (salinity) and permeability, but we are confident that the resistivity contrasts of the images are best interpreted principally as a grain-size phenomenon.

The image interpretation approach adopted here differs in some respects from previously published approaches (e.g. Serra 1989; Harker *et al.* 1990). We have extended Serra's (1989) Grade 1–3 categories of interpretation by adding grades 4 and 5 (Table 1), and shown examples of these in the following section.

Application to ODP Leg 129

The value of the FMS as an aid to the interpretation of poorly-recovered coring intervals is

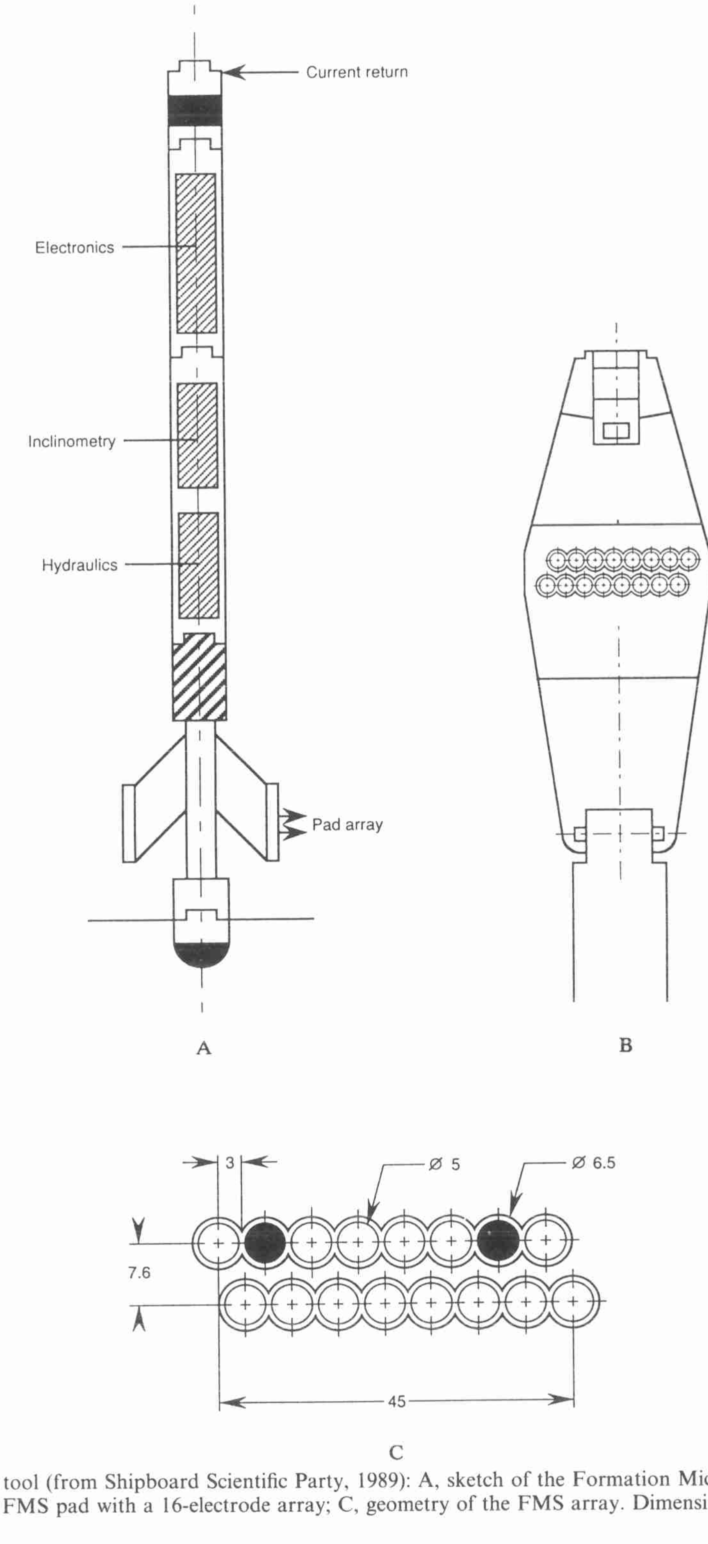

Fig. 3. FMS tool (from Shipboard Scientific Party, 1989): A, sketch of the Formation MicroScanner; B, sketch of an FMS pad with a 16-electrode array; C, geometry of the FMS array. Dimensions are in millimetres.

Table 1. *Categories of FMS image interpretation proposed in this study (modified from Serra 1989)*

Grade 1 (self-interpretable)	*Unique features, interpretable by themselves*	*Application in this study*
	beds, lamination, cross-lamination, grain-size and shape, grading, erosional surfaces, load clasts, slumps, microfolds, faults, burrows (± bioturbation)	most of these unique features recognized in non-recovered, poorly-recovered and disturbed intervals
Grade 2 (ambiguous)	*Ambiguous features, interpretable with the help of other log data*	*Application in this study*
	distinction between conglomerate/breccia pebbles, mud-shale clasts, concretions and bioturbation clarification of indistinct bedding, lamination and grading	although not discussed in this paper, dipmeter resistivity logs have been found the most useful for identifying different facies, with the aid of FMS images, in Leg 129 sites where no core exists
Grade 3 (unclear)	*Unclear features, interpretable with the help of core data from adjacent intervals*	*Application in this study*
	clarification of features listed in Grade 1 above where they are indistinct, weakly developed or on a very fine scale distinction between pebbles, mud clasts, concretions and bioturbation (as for Grade 2 images) identification of limestone textures and stylolites	interpretation of bioturbation, grading and slumping has been made in non-recovered and disturbed intervals
Grade 4 (unclear)	*Unclear features, interpretable with the help of core data/image calibration from a remote interval*	*Application in this study*
	as for Grade 3 above, but interpretation less certain because of lack of core data from adjacent intervals	interpretation of graded bedding, graded stratification and slumping has been made in disturbed and non-recovered intervals
Grade 5 (interpretable by association)	*Ambiguous features, interpretable by their close association with Grade 1 images*	*Application in this study*
	as for Grade 3 above, but interpretation by association with adjacent self-interpretable features	interpretation of grading, bioturbation, slumping and debris flows has been made in poorly-recovered, disturbed and non-recovered intervals

illustrated with reference to four specific problems from ODP Leg 129.

Poorly-recovered coring interval

This coring interval (core 129-802A-20R, 168.3–177.6 mbsf) is 9.7 m thick but core recovery is only 2.9%. The recovered sediments are mainly composed of fine sand to clay size volcanic glass and smectite/chloritic clays, with an average grain density of 2.82 g/cm^3, 44.6% porosity and 22.4% water content. From these few recovered pieces of bioturbated mud/sandstone (Fig. 4), it is not possible to reconstruct sedimentary facies, features and the type of bedding sequence for the entire coring interval. However, the FMS images over a part of this interval (Fig. 5) show the presence of three more or less distinct beds. The lowermost bed has a sharp, slightly irregular base, and grades upwards from light to very dark grey. A mottled or patchy aspect is evident in the top two-thirds of the bed. These features are most readily interpreted as representing a graded and deeply bioturbated turbidite (Serra 1989; Harker *et al.* 1990).

The middle bed appears to have a sharp planar base (although there seems to be some

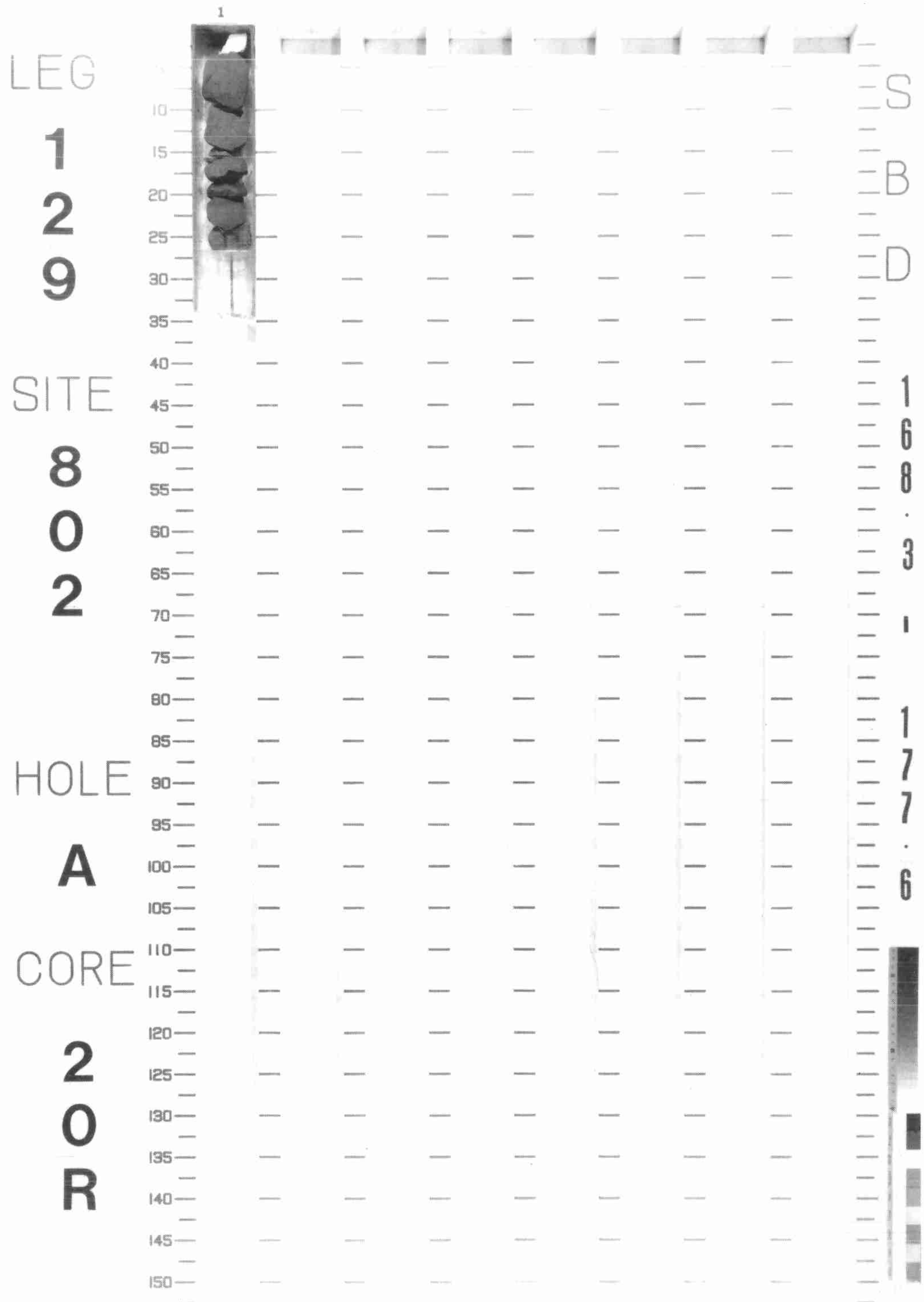

Fig. 4. Core photograph of the poorly-recovered coring interval (core 129-802A-20R).

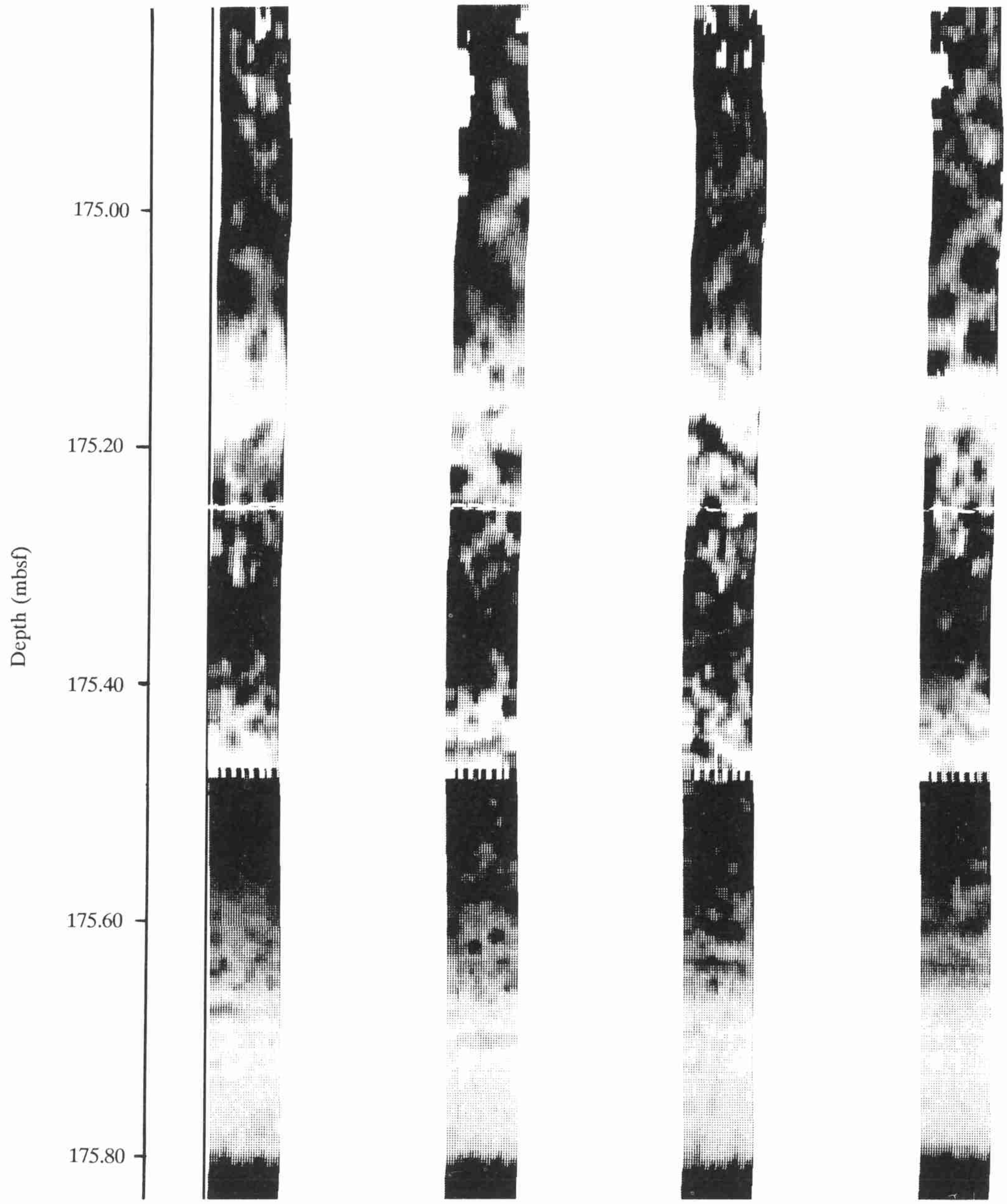

Fig. 5. Characteristic four-pad FMS images (scale 1:5, dynamic normalization, window = 30 cm) of turbidite beds encountered within the coring interval as mentioned in Fig. 4.

image artifact at this point), and then grades upwards from white/light grey to very dark grey. There is then a mottled and/or gradational contact with the overlying 'bed', which again grades upwards from white to very dark grey. The apparent oscillation-type grading and continuous mottling (bioturbation) through at least 1 m of section, superimposed upon episodic (turbiditic) supply, suggests that the uppermost bed and perhaps, the middle bed are best interpreted as hemiturbidites (Stow & Wetzel 1990). These are believed to be characteristic of distal turbidite/

basinal settings where the very slow settling of pelagic and turbiditic material allows for bioturbation to continue throughout deposition. This is periodically interrupted by the arrival of a more distinct turbidite unit.

The distinct graded to bioturbated bed at the base of image in Fig. 5, we believe, is a unique feature interpretable by itself, especially with prior knowledge of the local geological setting, and we would consider it a Grade 1 feature. This bed is one of many similar graded-to-bioturbated beds (17–115 cm thick) throughout the 9.7 m coring interval (Fig. 6). These have also been interpreted directly from the FMS images (Grade 1). The very limited core recovery shows clear bioturbation, so that interpretation of the bioturbated aspect throughout and the hemiturbidite at the top and middle of Fig. 5 would be considered a Grade 3 feature.

Coring interval showing drilling-induced disturbance

The coring interval (129-802A-14R) is 7.7 m thick with a moderately good recovery of 43.77%. However, the recovered portions (Fig. 7) are badly abraded by drilling, so that the sedimentary features are largely obscured. The sediments are mainly medium- to coarse-grained volcaniclastic sands with some granule-size clasts (mudclasts) and having a grain density of 2.65 g/cm^3, 31.3% porosity and 14.9% water content. Some sedimentary features are visible including stratification and a sharp bedding contact overlain by subtle graded bedding (Fig. 7), but our interpretation of the non-recovered interval has relied mainly on the calibration of FMS images with cores from other parts of the borehole, in cases where the images are not Grade 1 or 2.

Within this interval we can identify five main types of images or image facies (Fig. 8), which can be interpreted in terms of sedimentary structures. These are as follows:

(a) Light grey becoming progressively darker upwards (the vertical lines are an image artifact) (Fig. 8A). This is a rather subtle or unclear resistivity change which we interpret as graded bedding, at the base of a 1 m thick turbidite, on the basis of core/image calibration from another part of the borehole. The interpretation can therefore be assigned to a Grade 4 degree of confidence.

(b) Interlayered dark and light grey bands showing both gradational and mottled contacts (Fig. 8B). There would appear to be two possible interpretations of this feature: either it represents a series of thin–medium weakly graded beds with some bioturbation, or it is part of a coarsely-stratified, very thick-bedded turbidite in which the mottling is probably due to granules or cobbles and the stratification to grain size variation. We favour the latter interpretation (Grade 4 degree of confidence), partly because it is possible to recognize the very thick graded bed on the FMS images.

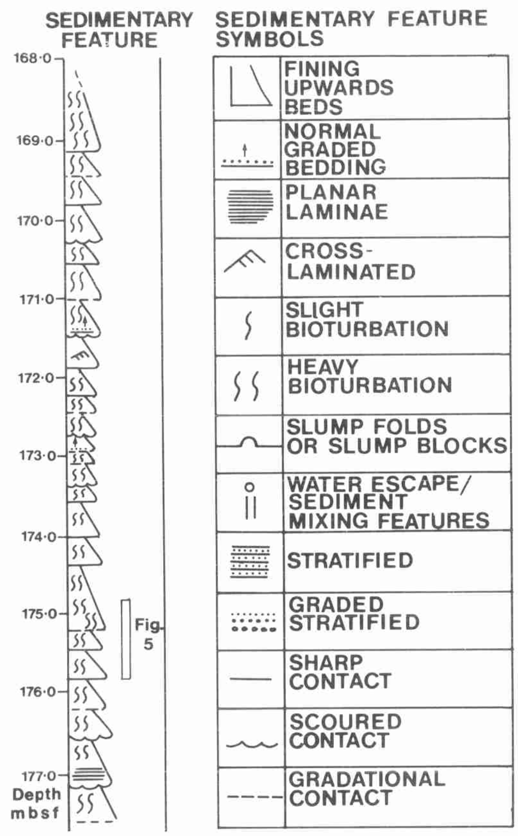

Fig. 6. Vertical sequence of sedimentary features of the coring interval as mentioned in Fig. 4.

(c) Interlayered, distinct dark and light grey bands with irregular contacts; plus some indistinct banding (Fig. 8C). This is best interpreted as a coarse stratification, rather than thin bedding, and is closely comparable to the centimetric stratification observed in the recovered core (Fig. 7, section 1, 62–67 cm), hence giving a Grade 3 degree of confidence to the interpretation. It lies just above the section illustrated in Fig. 8B, forming the upper part of the same thick graded bed.

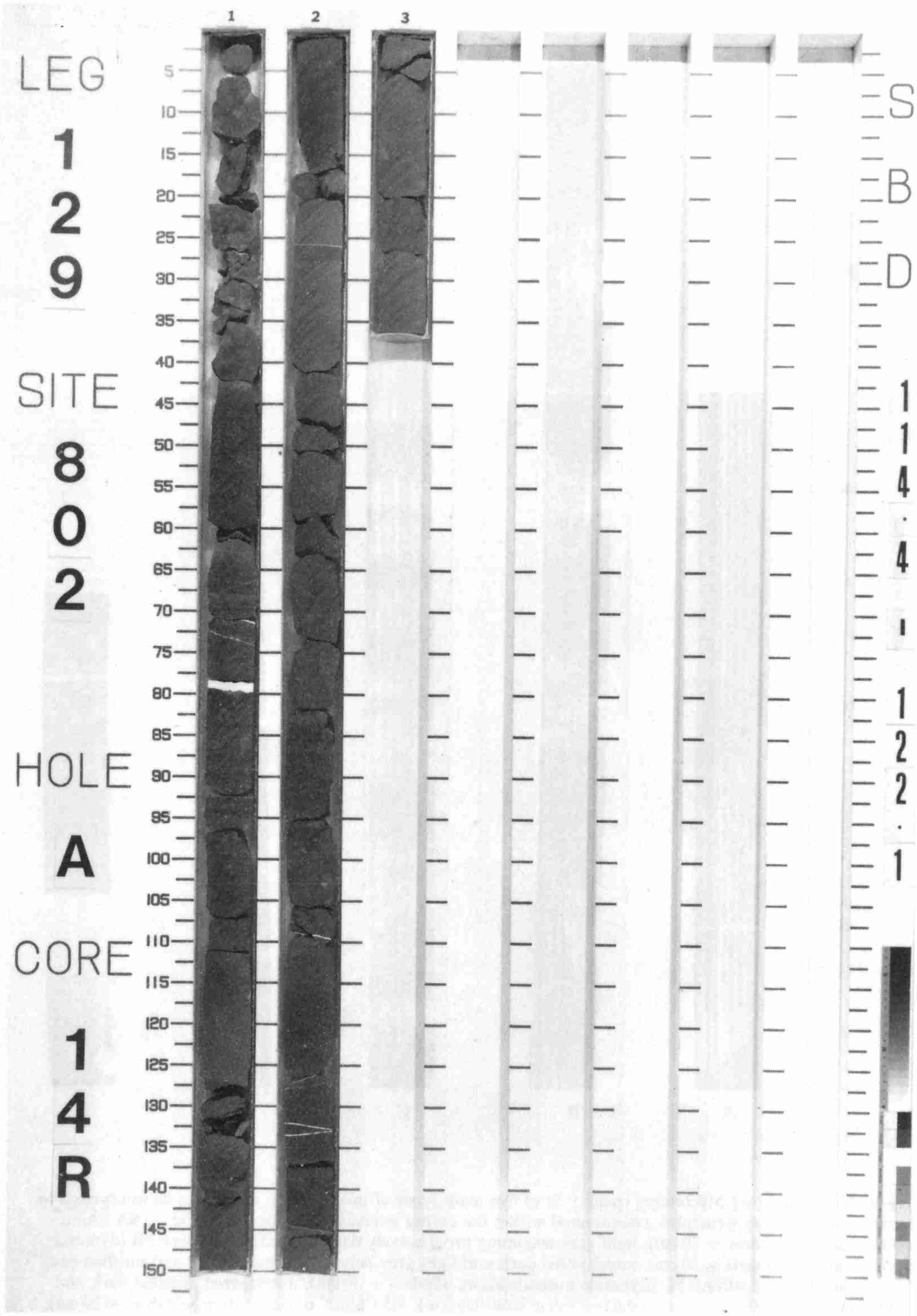

Fig. 7. Core photograph of the disturbed (drilling induced) coring interval (core 129-802A-14R).

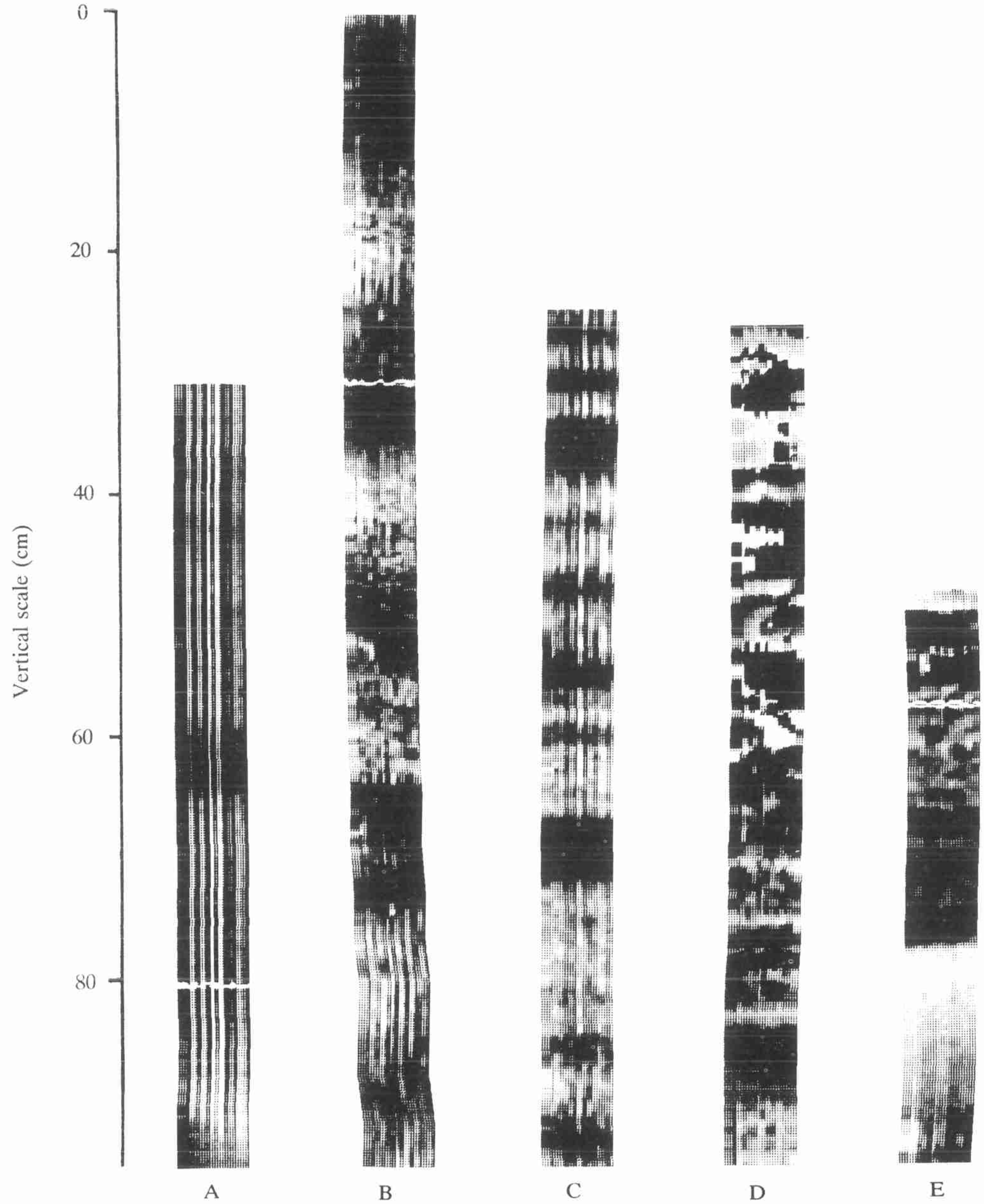

Fig. 8. Characteristic FMS images (scale 1:5) of five main types of image facies, which can be interpreted in terms of sedimentary structures, encountered within the coring interval as mentioned in Fig. 7: 8A ('hilite' normalization, window = 20 cm), light grey becoming progressively darker (graded bedding); 8B (dynamic normalization, window = 30 cm), interlayered dark and light grey bands with gradational and mottled contacts (graded stratification); 8C (dynamic normalization, window = 30 cm), interlayered, distinct dark and light grey bands with irregular contacts (coarse stratification); 8D ('hilite' normalization, window = 20 cm), stratified and cross-stratified interlayering of dark and light grey bands (parallel and cross-stratification); 8E (dynamic normalization, window = 30 cm), mottled aspect near top of section (bioturbation).

(d) Stratified and cross stratified interlayering of dark and light grey bands (Fig. 8D). This is readily interpreted as parallel and cross stratification within a thick bed, and with a Grade 1 degree of confidence.

(e) Mottled aspect near top of section (Fig. 8E). This appears to be part of a graded (lower part) to indistinctly laminated (middle part) to bioturbated (mottled upper part) turbidite bed, so we therefore interpret the mottling as bioturbation from its association with adjacent images (Grade 5 degree of confidence).

The interpreted sequence through the full 7.7 m coring interval is shown in Fig. 9, together with the location of the image facies illustrated in Fig. 8.

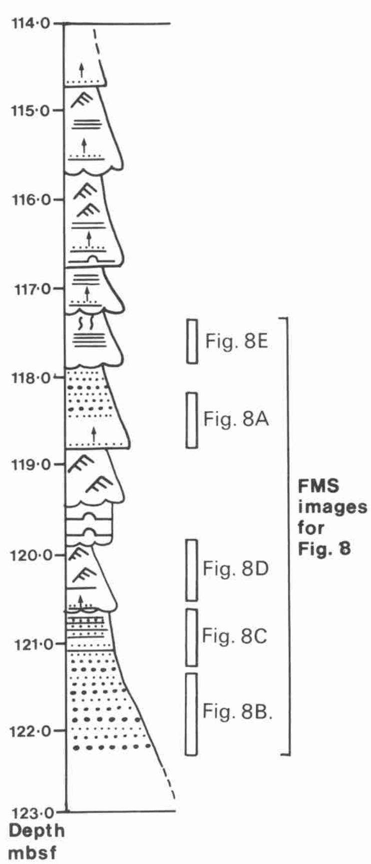

Fig. 9. The interpreted sequence (for key see Fig. 6) of the coring interval as mentioned in Fig. 7, together with the location of the image facies illustrated in Fig. 8.

Non-recovered coring interval

The coring interval 129-801B-9R (262.3–272.0 mbsf) has zero recovery over a section 9.7 m thick. The FMS images from this interval can be divided into three image facies on the basis of the geometry of resistivity events and texture of the images, and these can be interpreted in terms of sedimentary structures representing three different sedimentary facies.

(a) Interlayered light and dark grey bands, variably inclined, lenticular and with evidence of folding (Fig. 10A). The inclined layering and microfolds (recumbent) are clearly interpretable in terms of a slump unit, showing considerable internal contortion (a Grade 1 feature).

(b) Irregular light and dark grey bands, with possible evidence of folding (Fig. 10B). The microfolds together with a somewhat chaotic sediment mixing suggest almost certainly a slump unit, showing less internal contortion than (a) above (Grade 1). However, if we are more cautious in applying a direct image interpretation, we might assign it a Grade 3/4 (comparison with other cored sections) or Grade 5 (association with Grade 1 images) category.

(c) Irregular mottling of light and dark grey (Fig. 10C). Such mottling might be caused by pebbles within a conglomerate, mud clasts, concretions or bioturbation. In this case, however, we favour the complete disruption of interbedded sand and mud units (light and dark greys) and transport/deposition by debris flow, so that the mottling is interpreted as variable lithologies/clasts within a debrite. The larger patches towards the top of the image (Fig. 10C) may represent either large clasts or a gradational transition to an overlying (?) slumped unit. This interpretation is made both by reference to core data from adjacent intervals (Grade 3 feature) and by association with Grade 1 images of slumps (Grade 5 feature).

The full coring interval is shown interpreted in Fig. 11. The gradational contacts between slump and debrite units may indicate the transformation of slumping into debris flow processes.

Location of cores in well-recovered coring intervals

The cored interval 129-801B-1R has a recovery of about 67.73% over 9.5 m of section. From the core photograph (Fig. 12) it can be seen that the interval has encountered two sedimentary facies: one (section 1, 186.0–186.80 mbsf) consists of laminated sandstones and the other (section

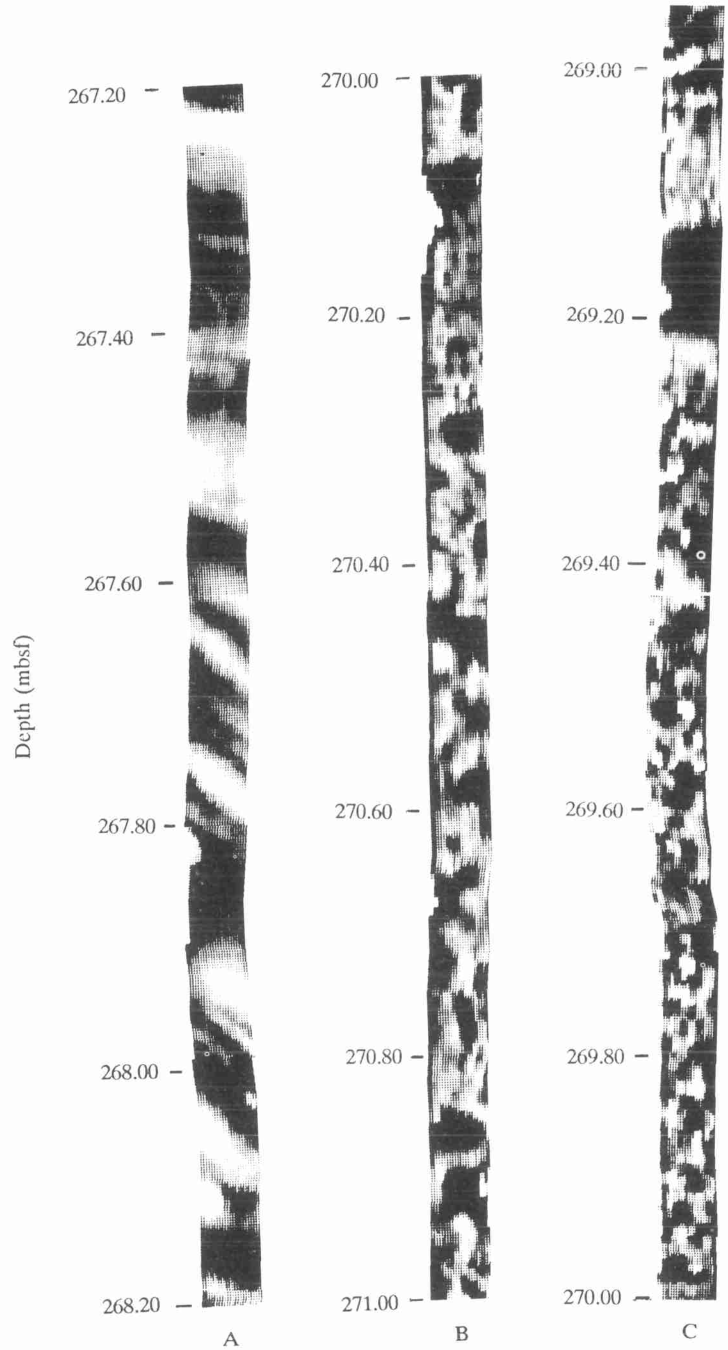

Fig. 10. FMS image facies (scale1:5) representing three different sedimentary facies within the non-recovered coring interval (core 129-801B-9R): 8A ('hilite' normalization, window = 20 cm), interlayered light and dark grey bands, variably inclined, lenticular and with folding, 8B (dynamic normalization, window = 10 cm), irregular dark and light grey patches, with evidence of possible folding and somewhat chaotic sediment mixing; 8C (dynamic normalization, window = 10 cm), irregular mottling of light and dark grey, which might be caused by variable lithologies/clasts within a debrite.

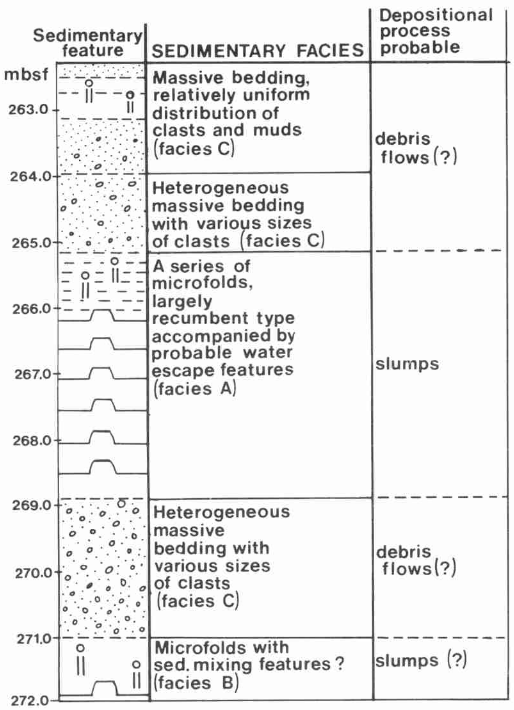

Fig. 11. The interpreted sequence (for key see Fig. 6) of the coring interval as mentioned in Fig. 10.

1-cc, 186.80–195.5 mbsf) of massive structureless sandstones. The FMS images also reveal the presence of these two facies within the coring interval precisely and calibrated image facies are shown in Fig. 13. Since recovered sections are conventionally located at the top of the cored interval, the laminated facies has been located in the upper 80 cm of section 1. However, the FMS images show that the laminated interval is, in fact, 2 m thick starting from the topmost part of the cored section, that is from 186 m to 188 m. This implies that part of the missing core is from the top 2 m of the cored interval, and not from the base as convention dictates. The location of the rest of the missing core is not possible to determine as the FMS images show the underlying 7.5 m to be entirely of massive structureless sandstones with varying degree of heterogeneity.

Discussion and conclusion

Core recovery at ODP Leg 129 sites typically ranged from 17.3 to 29.5%, but is 0–5% in a number of cored intervals. In many cases, even the recovered cores are badly disturbed, abraded, fragmented and brecciated by drilling disturbance. This situation is common in ODP holes, whereas many oil exploration wells are only spot cored if cored at all.

With the aid of a good suite of FMS logs, computer processing, image enhancement, and at least some core recovery to allow calibration, it has been possible to obtain information concerning the sediment from intervals with poor or zero core recovery. The correct location of recovered portions of core within a longer cored interval may also be estimated given that distinctive sedimentary features can be recognized in both core and image. Where parts of cores show signs of disturbance, comparison with the FMS image may allow distinction between drilling-induced effects and those of sedimentary origin.

The interpretation approach used has followed that of previous studies (e.g. Serra 1989; Harker *et al.* 1990), although the sediments described in this study are all of volcaniclastic origin and therefore provide new documentation of FMS images for this class of sediment. Calibration of images with well-recovered coring intervals has shown that resistivity contrasts on images are most closely related to grain-size changes in the sediment.

Furthermore, we have found it helpful to extend Serra's (1989) scheme for the grading of image interpretation, with the addition of two further grades: Grade 4 for unclear features interpretable with the help of core/image data from a remote interval or borehole, and Grade 5 for ambiguous features interpretable by association with Grade 1 images. Harker *et al.*'s (1990) grading scheme does not compare directly with that of Serra (1989), apart from their Grade 1 images, and we have found it to be less helpful.

The sedimentological data gained from this detailed FMS study of ODP Leg 129 volcaniclastics has been extremely beneficial to our understanding of basin development in this part of the Pacific as well as to better characterization of sedimentary structures in volcaniclastic turbidites and associated facies. It has been possible to demonstrate the existence of slumps and of slump–debrite couplets, and to determine a sequence of structures through thick-bedded, coarse-grained, volcaniclastic turbidites. In addition, it may be possible to recognize distinct ichnofacies within these sediments using enhanced FMS images and careful selection of window size during processing.

The primary data were collected during ODP Leg 129 on which one of the authors (ARMS) was a participant. The ODP staff and the captain, officers and crew of *Joides Resolution* are thanked for their part in this

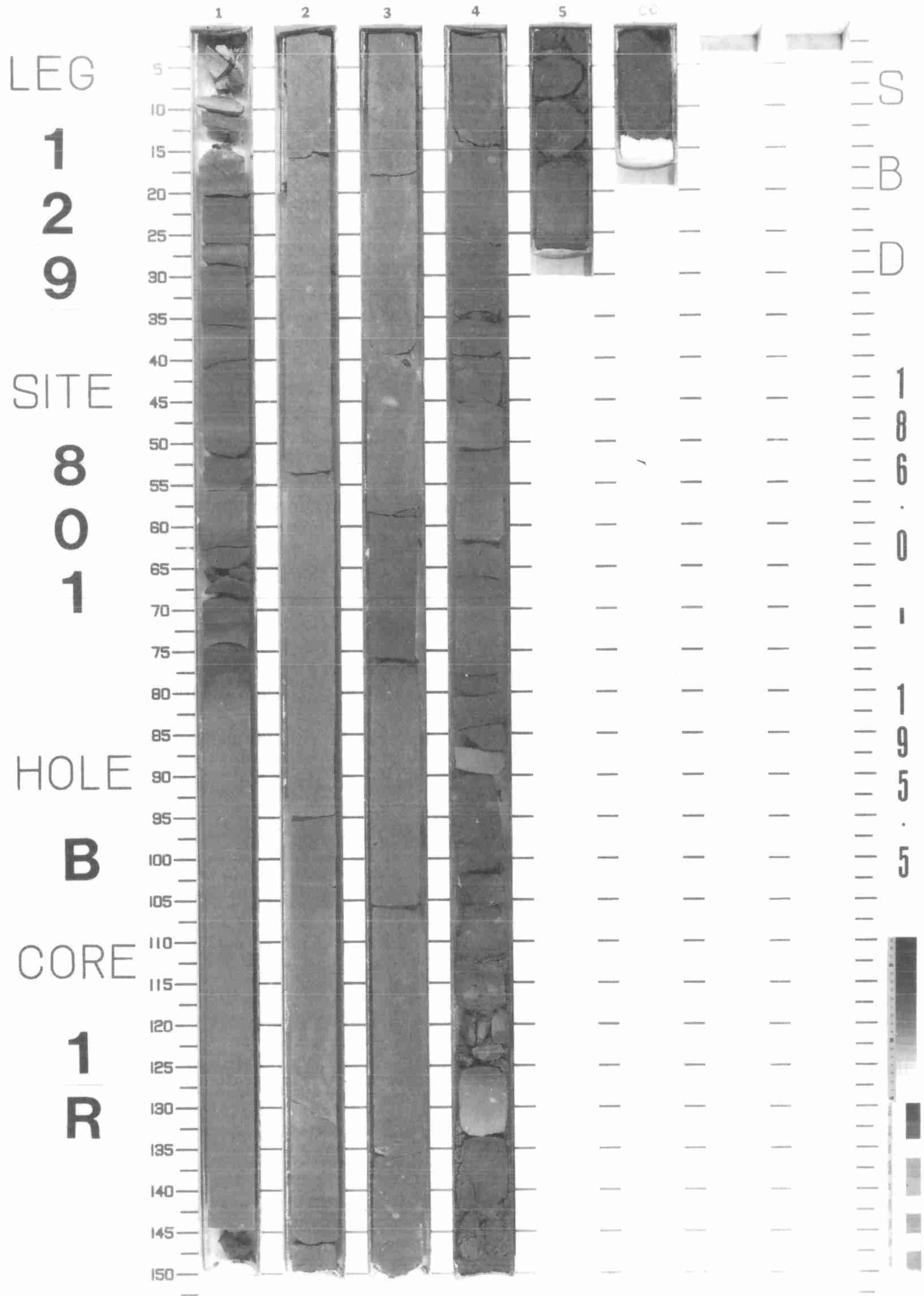

Fig. 12. Core photograph of the well recovered coring interval (core 129-801B-1R) showing the presence of two sedimentary facies: laminated (subtle) sandstones (upper portion of section-1) and structureless massive sandstones with some larger clasts in places.

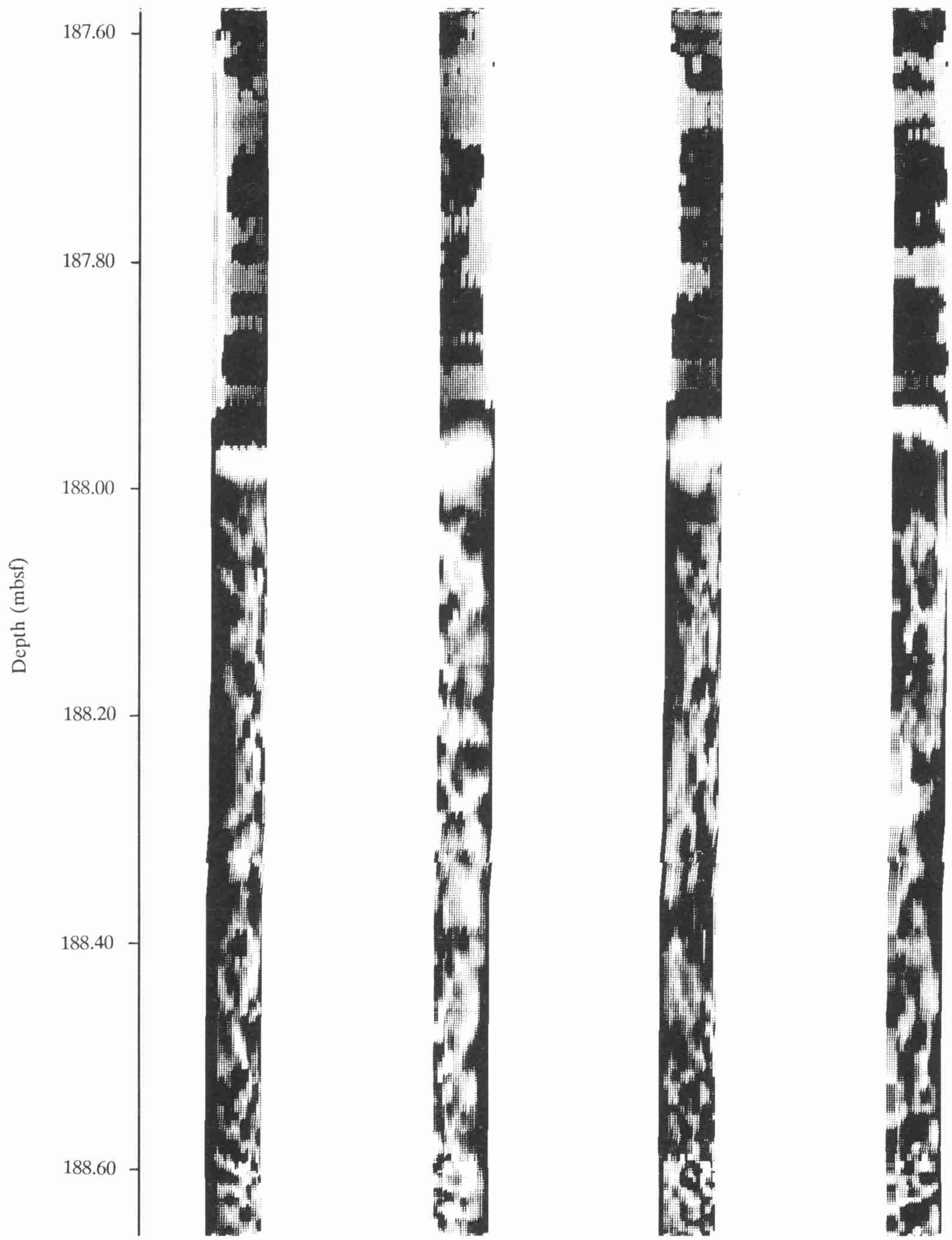

Fig. 13. Four pad FMS images (scale 1:5, 'hilite' normalization, window = 20 cm) showing the presence of two sedimentary facies: laminated (subtle) sandstones (section above 188 mbsf) and structureless massive sandstones (section below 188 mbsf).

cruise. We are also very grateful for the technical help from the Borehole Research Group and especially from Robin Reynolds during the processing of the FMS images at the Lamont Doherty Geological Observatory. Staff in the Geology Department of Southampton University are thanked for their help in the final preparation of this paper.

References

EKSTROM, M. P., DAHAN, C., CHEN, M.-Y., LLOYD, P. & ROSSI, D. J. 1987. Formation imaging with microelectrical scanning arrays. *The Log Analyst*, **28**, 294–306.

HARKER, S. D. *et al.* 1990. Methodology of formation micro-scanner image interpretation in Claymore and Scapa Fields (North Sea). *In*: HURST, A., LOVELL, M. A. & MORTON, A. C. (eds) *Geological Applications of Wireline Logs*. Geological Society, London, Special Publication, **48**, 13–23.

LARSON, R. L., PITMAN, W. C., GOLOVCHENKO, X., CANDE, S. C., DEWEY, J. F., HAXBY, W. F. & LABRECQUE, J. L. 1985. *The Bedrock Geology of the World*. Freeman, New York.

Shipboard Scientific Party, 1990. *In*: LANCELOT, Y. V. & LARSON, R. *et al. Proceedings of the Ocean Drilling Program, Initial Reports*. Ocean Drilling Program, College Station, TX, **129**, 26, 34.

Shipboard Scientific Party, 1989. Site 787. *In*: TAYLOR, B., FUJIOKA, K. *et al. Proceedings of the Ocean Drilling Program, Initial Reports*. Ocean Drilling Program, College Station, TX, **126**, 39–41.

SERRA, O. 1989. *Schlumberger Formation Microscanner Image Interpretation* Schlumberger Education Services, 16–96.

STOW, D. A. V. & WETZEL, A. 1990. Hemiturbidite: a new type of deep-water sediment. *In*: COCHRAN, J. R., STOW, D. A. V. *et al. Proceedings of the Ocean Drilling Program, Scientific Results*. Ocean Drilling Program, College Station, TX, **116**, 25–34.